

## Binding investigation and preliminary optimisation of the 3-amino-1,2,4-triazin-5(2H)-one core for the development of new Fyn inhibitors

Giulio Poli<sup>a</sup>, Margherita Lapillo<sup>a</sup>, Carlotta Granchi<sup>a</sup> , Jessica Caciolla<sup>a</sup>, Nayla Mouawad<sup>a,b</sup>, Isabella Caligiuri<sup>b</sup>, Flavio Rizzolio<sup>b,c</sup> , Thierry Langer<sup>d</sup>, Filippo Minutolo<sup>a</sup>  and Tiziano Tuccinardi<sup>a,e</sup> 

<sup>a</sup>Department of Pharmacy, University of Pisa, Pisa, Italy; <sup>b</sup>Pathology Unit, Department of Molecular Biology and Translational Research, National Cancer Institute and Center for Molecular Biomedicine, Aviano (PN), Italy; <sup>c</sup>Department of Molecular Science and Nanosystems, Ca' Foscari Università di Venezia, Venezia-Mestre, Italy; <sup>d</sup>Department of Pharmaceutical Chemistry, Faculty of Life Sciences, University of Vienna, Vienna, Austria; <sup>e</sup>Sbarro Institute for Cancer Research and Molecular Medicine, Center for Biotechnology, College of Science and Technology, Temple University, Philadelphia, PA, USA

### ABSTRACT

Fyn tyrosine kinase inhibitors are considered potential therapeutic agents for a variety of human cancers. Furthermore, the involvement of Fyn kinase in signalling pathways that lead to severe pathologies, such as Alzheimer's and Parkinson's diseases, has also been demonstrated. In this study, starting from 3-(benzo[d][1,3]dioxol-5-ylamino)-6-methyl-1,2,4-triazin-5(2H)-one (**VS6**), a hit compound that showed a micromolar inhibition of Fyn ( $IC_{50} = 4.8 \mu M$ ), we computationally investigated the binding interactions of the 3-amino-1,2,4-triazin-5(2H)-one scaffold and started a preliminary hit to lead optimisation. This analysis led us to confirm the hypothesised binding mode of **VS6** and to identify a new derivative that is about 6-fold more active than **VS6** (compound **3**,  $IC_{50} = 0.76 \mu M$ ).

### ARTICLE HISTORY

Received 21 March 2018  
Revised 20 April 2018  
Accepted 21 April 2018



### KEYWORDS


Fyn kinase; molecular modelling; kinase inhibitors; drug design

### Introduction

Fyn kinase is a member of the Src family kinases (SFKs), which is one of the largest and most studied families of non-receptor tyrosine kinases (TKs) due to the implications of its members in oncogenesis and cancer development. Fyn kinase is involved in a plethora of physiological processes ranging from cell growth, adhesion and motility to ion channels and platelet activation, as well as cytokine receptor and growth factor signaling<sup>1</sup>. At the level of the central nervous system (CNS), Fyn exerts several different functions connected to brain development. In fact, Fyn is involved in axon–glial signal transduction, oligodendrocyte maturation and myelination<sup>2</sup>; it also stimulates the synthesis of abundant myelin associated oligodendrocytic basic protein, thus influencing oligodendroglial morphological differentiation<sup>3</sup>, and it is implicated in synapse formation and post-synaptic excitatory transmission<sup>4</sup>. Moreover, Fyn was found to be implied in T-cell development, homeostasis, activation and to have a critical role in thymocyte development together with Lck kinase, which is another member of the SFKs<sup>5</sup>. Due to its several physiological roles, an aberrant expression of Fyn kinase or a dysregulation of its activity is involved in the development and progression of different pathological conditions. In fact, Fyn overexpression has been connected to the pathogenesis of various types of tumors<sup>1</sup>, particularly prostate<sup>6</sup>, breast<sup>7</sup> and ovarian cancer<sup>8</sup>, as well as haematological tumours like chronic myeloid leukemia<sup>9</sup> and other types of cancer like glioblastoma and neuroblastoma<sup>10</sup>. Moreover, recent studies highlighted the role of Fyn in the resistance of some tumour cells to anti-cancer treatments, such as in tamoxifen-resistant breast

cancer cell lines<sup>11</sup>. Recently, Fyn kinase gained more and more attention as a new therapeutic target for the treatment of neurodegenerative pathologies. Fyn plays a key role in the development and progression of Alzheimer's disease (AD), being involved in the synaptic toxicity and cognitive impairments produced by amyloid- $\beta$  ( $A\beta$ ) oligomers and promoting the formation of neurofibrillary tangles by phosphorylating Tau protein<sup>12</sup>. In fact, Fyn kinase,  $A\beta$  and Tau protein have been even referred to as the “toxic triad” of AD. Furthermore, Fyn showed to be a mediator of the microglial neuroinflammatory processes typical of Parkinson's disease (PD) and could thus represent a potential target for the treatment of neurodegenerative diseases that, like PD, are associated with proinflammatory processes involving microglia. Due to its involvement in cancer and CNS pathologies, the identification of selective Fyn inhibitors is an expanding field of study. Several TKs small-molecule inhibitors with activity towards Fyn kinase have been reported in literature<sup>13</sup>. However, potent Fyn inhibitors with high selectivity over other TKs and, in particular, over the other SFKs members are still missing. As an example, the well-known pyrazolo[3,4-*d*]pyrimidine **PP2**, is a low nanomolar inhibitor of Fyn kinase identified by Hanke and collaborators in 1996<sup>14</sup>, which is still commonly used to study the complex network of physiological processes involving Fyn kinase activity<sup>15–17</sup>. Nevertheless, **PP2** is also endowed with a comparable inhibitory activity towards other SFKs, in particular Src and Lck, and demonstrated to be remarkably potent also on other kinases such as CK1 $\delta$  (Casein kinase 1  $\delta$ ), RIP2 (receptor-interacting protein kinase 2) and GAK (cyclin G-associated kinase)<sup>18</sup>. Virtual screening (VS) approaches have shown to be a powerful tool for the discovery of new Fyn kinase

**CONTACT** Tiziano Tuccinardi  [tiziano.tuccinardi@unipi.it](mailto:tiziano.tuccinardi@unipi.it)  Department of Pharmacy, University of Pisa, Via Bonanno 6, 56126 Pisa, Italy

 Supplemental data for this article can be accessed [here](#).

© 2018 The Author(s). Published by Informa UK Limited, trading as Taylor & Francis Group.

This is an Open Access article distributed under the terms of the Creative Commons Attribution License (<http://creativecommons.org/licenses/by/4.0/>), which permits unrestricted use, distribution, and reproduction in any medium, provided the original work is properly cited.

and SFKs inhibitors<sup>19</sup>. In particular, we recently developed a VS study mixing ligand-based and receptor-based approaches, which allowed the identification of a novel small-molecule inhibitor of Fyn kinase (compound **VS6**) with low micromolar potency<sup>20</sup>. Here, we report the computational investigation of **VS6** binding mode into Fyn catalytic site, carried out through consensus docking, MD simulations and binding free energy evaluations, followed by a preliminary structural optimisation aimed at the development of novel potent Fyn inhibitors.

## Materials and methods

### Molecular modelling

#### Consensus docking studies

The ligands were built by means of Maestro<sup>21</sup> and were then minimised in a water environment (using the generalised Born/surface area model) by means of MacroModel<sup>22</sup>. The minimisation was performed using the conjugate gradient (CG), the MMFFs force field, and a distance-dependent dielectric constant of 1.0 until the ligands reached a convergence value of 0.05 kcal Å<sup>-1</sup> mol<sup>-1</sup>. Nine different docking procedures were applied and for each docking calculation only the best scored pose was taken into account<sup>23–25</sup>. The docking calculations were carried out by using AUTODOCK 4.2.3<sup>26</sup>, DOCK 6.7<sup>27</sup>, FRED 3.0<sup>28–31</sup>, GOLD 5.1 (with the ASP, CSCORE and GSCORE scoring functions)<sup>32</sup>, GLIDE 5.0 (with the SP scoring function)<sup>33</sup>, AUTODOCK VINA 1.1<sup>34</sup>, and PLANTS<sup>35</sup> accordingly employing the procedures previously described<sup>24,36</sup>. The ligands were docked into the binding site of human Fyn (2DQ7<sup>37</sup> PDB code) by using the different docking procedures, then the root mean square deviation (RMSD) of each of these docking poses against the remaining docking results was evaluated using the rms\_analysis software of the GOLD suite. The most populated cluster of solutions was then considered and subjected to molecular dynamic (MD) simulations.

**MD simulations.** All simulations were performed using AMBER, version 14<sup>38</sup>. MD simulations were carried out using the ff14SB force field at 300 K in a rectangular parallelepiped water box. The TIP3P explicit solvent model for water was used. Chlorine ions were added as counter ions to neutralise the system. Prior to MD simulations, two steps of minimisation were carried out using the same procedure described above. Particle mesh Ewald (PME) electrostatics and periodic boundary conditions were used in the simulation<sup>39</sup>. The time step of the simulations was 2.0 fs with a cut-off of 10 Å for the non-bonded interactions, and SHAKE was employed to keep all bonds involving hydrogen atoms rigid. Constant volume periodic boundary MD was carried out for 0.5 ns, during which the temperature was raised from 0 to 300 K. Then, 99.5 ns of constant pressure periodic boundary MD was carried out at 300 K using the Langevin thermostat to maintain constant the temperature of our system. All the  $\alpha$  carbons of the protein were blocked with a harmonic force constant of 10 kcal/mol·Å<sup>2</sup>. General Amber force field (GAFF) parameters were assigned to the ligands, while partial charges were calculated using the AM1-BCC method as implemented in the Antechamber suite of AMBER 14.

#### Binding energy evaluation

The evaluation of the binding energy associated with the ligand–protein complexes analysed through MD simulations was carried out using AMBER 14. The trajectories relative to the last 50 ns of each simulation were extracted and used for the calculation, for a total of 50 snapshots (at time intervals of 1 ns). Van der Waals,

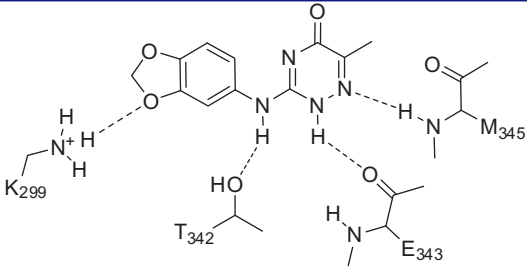
electrostatic and internal interactions were calculated with the SANDER module of AMBER 14, whereas polar energies were calculated using both the Generalised Born and the Poisson – Boltzmann methods with the MM-PBSA module of AMBER 14. Dielectric constants of 1 and 80 were used to represent the gas and water phases, respectively, while the MOLSURF program was employed to estimate the non-polar energies.

**Fyn kinase assays.** Compound **1** was synthesised, compounds **2** and **3** were purchased from Vitas-M Laboratory, whereas **PP2** was purchased from Tocris Bioscience. Full-length recombinant human Fyn, Poly(Glu4, Tyr1) synthetic peptide substrate, ATP stock solution and Kinase-Glo<sup>®</sup> Luminescent Kinase Assay were purchased from Promega. The kinase reaction was conducted at room temperature at a final volume of 50  $\mu$ L in 40 mM Tris buffer, pH 7.5, containing 20 mM MgCl<sub>2</sub> and 0.05 mM DTT. A total of 10  $\mu$ L of ATP 20  $\mu$ M were added to 10  $\mu$ L of Poly(Glu4, Tyr1) synthetic peptide substrate 1  $\mu$ g/ $\mu$ L and 5  $\mu$ L of DMSO containing the appropriate amount of compound. The reaction was initiated by the addition of 25  $\mu$ L of Fyn (36–48 ng/well) in such a way that the assay was linear over 60 min. The final concentration of the analysed compounds ranged from 10 to 0.032  $\mu$ M for **PP2** and from 200 to 0.01  $\mu$ M for compounds **1–3**. After the reaction had proceeded for 60 min, 50  $\mu$ L Kinase-Glo<sup>®</sup> reagent was added to terminate the reaction. This solution was then allowed to proceed for additional 10 min to maximise the luminescence reaction. Values were then measured by using a VictorX3 PerkinElmer instrument for luminosity measurements. Two reactions were also run: one reaction containing no compounds and the second one containing neither inhibitor nor enzyme.

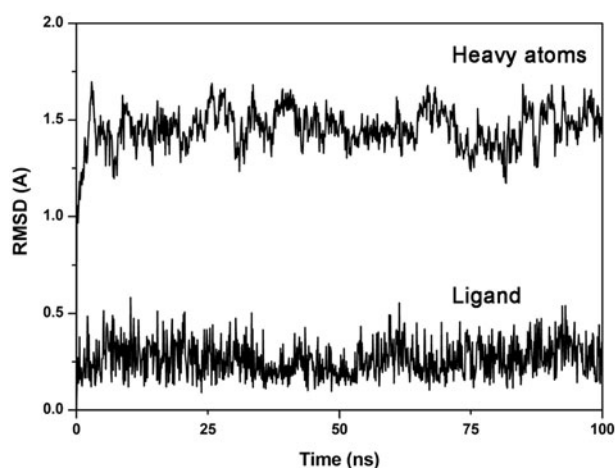
**Cell viability assay.** MDA-MB-231 (human breast carcinoma cells) and A549 (non-small cell lung cancer) were purchased from ATCC and maintained at 37 °C in a humidified atmosphere containing 5% CO<sub>2</sub> accordingly to the supplier. Cells (10<sup>3</sup>) were plated in a 96-well culture plates. The day after seeding, vehicle or compounds were added at different concentrations to the medium. Compounds were added to the cell culture at a concentration ranging from 200 to 0.1  $\mu$ M. Cell viability was measured after 96 h according to the supplier (Promega, G7571) with a Tecan M1000 instrument. IC<sub>50</sub> values were calculated from logistical dose response curves. Mean and standard deviation were reported ( $n=3$ ).

## Results and discussion

Recently, through a virtual screening (VS) study combining a FLAP ligand-based similarity analysis with docking and MD simulations, we identified few hit compounds endowed with low micromolar Fyn inhibitory potency<sup>20</sup>. Among these, compound **VS6**, (Table 1) bearing a 3-amino-1,2,4-triazin-5(2H)-one scaffold, showed the most interesting activity with an IC<sub>50</sub> value for Fyn inhibition of 4.8  $\mu$ M. With the aim of paving the way for the structural optimisation of the ligand and for the development of derivatives with higher affinity for Fyn kinase, consensus docking, MD simulations and relative binding free energy evaluations were used to assess the reliability of the binding mode predicted for compound **VS6** within Fyn catalytic site. As a first step of our analysis, compound **VS6** was subjected to our recently developed consensus docking approach combining different docking methods (see Materials and Methods for details), which was found to predict ligand binding poses better than the single docking procedures and to provide hints about binding pose reliability<sup>23,24</sup>. The consensus docking approach gave a first confirmation of the reliability of the binding

**Table 1.** H-bonds analysis of VS6 with Fyn during the MD simulation.


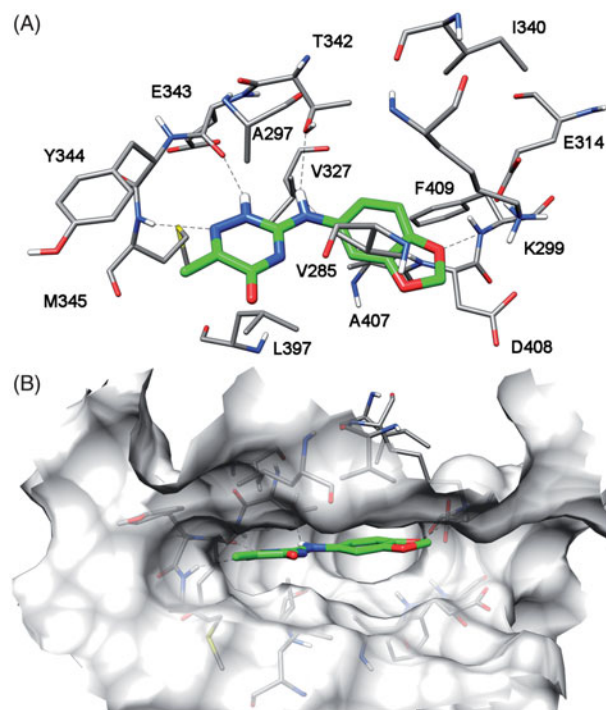
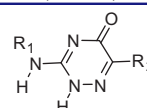
acceptor	donor H	donor	% occupied
E343@O	LIG@H	LIG@N5	96.7
LIG@N4	M345@H	M345@N	92.1
T342@OG1	LIG@H	LIG@N8	49.8
LIG@O12	K299@H	K299@NZ	21.6

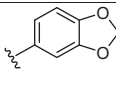
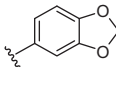
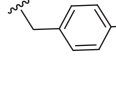
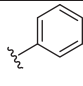
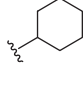
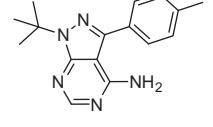
**Figure 1.** Analysis of the MD simulation of Fyn kinase in complex with VS6. The RMSD of the ligand and the heavy atoms of the receptor from the starting model structure during the simulation is reported.

disposition into Fyn kinase domain previously proposed for **VS6**, since 6 out of the 9 docking methods tested predicted the same result. The binding mode of compound **VS6** has been further analysed by subjecting this ligand–protein complex to 100 ns of MD simulation. By analysing the root-mean square deviation (RMSD) of all the heavy atoms from the X-ray structures, we observed an initial increase followed by a stabilisation of the RMSD value around 1.5 Å (Figure 1). Regarding the geometry of the ligand, we analysed the trend of the RMSD of its position over time during the simulation with respect to the starting docking pose, and it showed an average RMSD value of about 0.3 Å.

Figure 2 shows the suggested binding disposition of compound **VS6** refined through MD simulation. The triazinone central core of the compound interacts with the hinge region of the kinase forming two H-bonds with the nitrogen backbone of M345 and the oxygen backbone of E343. Concerning the substituents connected with this scaffold, the 6-methyl group does not show any important interaction and, as shown in Figure 2(B), it is directed outside the binding site towards the solvent exposed region of the protein; the amine group forms an H-bond with the hydroxyl group of T342, and the benzodioxole ring shows lipophilic interactions with V285 and A407 and it is positioned near the positive nitrogen of K299.

As shown in Table 1, the H-bond analysis of the MD simulation confirms the stability of the interactions with the backbone of E343 and M345 since during the whole simulation they are highly

**Figure 2.** Putative binding mode of compound VS6 into Fyn kinase. (A) View of the most relevant ligand–receptor interactions and (B) binding pose of the ligand (green) in the binding site.**Table 2.** Structure and Fyn inhibitory activity of the tested compounds.


	R <sub>1</sub>	R <sub>2</sub>	IC <sub>50</sub> (μM)
<b>VS6</b>		-CH <sub>3</sub>	4.8
<b>1</b>			5.2
<b>2</b>		-CH <sub>3</sub>	> 100
<b>3</b>		-CH <sub>3</sub>	0.76
<b>PP2</b>			0.061

conserved (92–97% occupied populations). Differently from these two interactions, the H-bonds with T342 and K299 are maintained only for 50–22% of the whole simulation.

As a further step of this research study, we were aimed at experimentally verifying the reliability of the proposed binding disposition. From a chemical point of view, the easiest way to

**Table 3.** H-Bonds analysis of compounds **2** and **3** with Fyn during the MD simulation.

acceptor	donor H	donor	% occupied
<b>Compound 2</b>			
E343@O	LIG@H	LIG@N5	99.6
LIG@N4	M345@H	M345@N	91.4
T342@OG1	LIG@H	LIG@N8	47.6
<b>Compound 3</b>			
E343@O	LIG@H	LIG@N5	99.9
LIG@N4	M345@H	M345@N	86.8
T342@OG1	LIG@H	LIG@N8	91.0

confirm this binding mode was the addition of a large substituent in the place of the methyl group in position 6 of the triazinone. As reported above, this methyl group is directed outside the binding site towards the solvent exposed surface of the protein; therefore, a substitution in this point of the molecule should not determine important variations of the compound inhibitory activity. Based on this hypothesis, compound **1**, characterised by the presence of a *p*-fluorobenzyl fragment in position 6 of the triazinone ring, was synthesised (see [Supplementary Material](#)) and tested for its inhibitory activity. As shown in [Table 2](#), this compound displayed an  $IC_{50}$  value very similar to that possessed by **VS6**, thus supporting the proposed binding hypothesis.

After having obtained the additional experimental support of the proposed **VS6** binding mode, we investigated the role of the aminobenzodioxole fragment. The MD simulation suggested that the amino group was able to interact with the hydroxyl fragment of T342; however, this interaction was not highly stable. A deep analysis of the simulation highlighted that the distance between the oxygen of T342 and the nitrogen of the amine was usually in the range values of an H-bond interaction. However, the conjugation of the amine group with the aromatic benzodioxole and the triazinone ring hindered the rotation of the torsions associated with the nitrogen, leading to a planar configuration of the benzodioxolylaminotriazinone. With this geometry, the amine moiety was not able to efficiently interact with the oxygen of T342, due to the donor–acceptor H-bond angle that showed an average value of about  $140^\circ$ . Concerning the benzodioxole ring, the MD simulation analysis shows lipophilic interactions and also an additional H-bond contribution for the interaction of this compound with K299. In order to evaluate the role of the T342 and K299 H-bonds with the ligand, the benzodioxole ring was replaced with a phenyl (compound **2**) and a cyclohexyl ring (compound **3**). These two compounds, which were not previously tested as inhibitors of Fyn or other kinases, were thus docked into the Fyn-binding site and then subjected to the MD simulation protocol applied for compound **VS6**. [Table 3](#) shows the H-bond analysis of the MD simulation for the two compounds; obviously, for both compounds there were no H-bond interactions with K299. Furthermore, in agreement with the planar geometry of the amine group of the ligand, compound **2** showed an H-bond interaction scheme similar to that showed by **VS6**, with two highly stable interactions with the backbone of E343 and M345 (91–100% occupied populations) and a less stable interaction with T342 (48%

**Table 4.** MM-PBSA results for the complexes of Fyn with **VS6** and compounds **2–3**.  $\Delta$ PBSA is the sum of the electrostatic (Ele), van der Waals (VdW), polar (PB) and non-polar (PBSur) solvation free energy. Data are expressed as  $\text{kcal}\cdot\text{mol}^{-1}$ .

	Ele	VdW	PBSur	PB	$\Delta$ PBSA
<b>VS6</b>	−27.5	−35.0	−3.1	36.5	−29.1
<b>2</b>	−26.5	−32.9	−2.8	34.9	−27.3
<b>3</b>	−28.5	−34.4	−3.0	33.5	−32.4

occupied population). The replacement of the aromatic ring with the cyclohexyl group should allow a level of amine torsional freedom greater than that possessed by **VS6**. Interestingly, as shown in [Table 3](#), all the three H-bond interactions formed by compound **3** were highly stable with occupancy values higher than 86%.

The three MD trajectories of compounds **VS6** and **2–3** were further analysed through the Molecular Mechanics–Poisson–Boltzmann Surface Area (MMPBSA) method<sup>40</sup> that has been shown to accurately estimate the ligand–receptor energy interaction<sup>41–45</sup>. This approach averages the contributions of gas-phase energies, solvation free energies and solute entropies calculated for snapshots of the complex molecule as well as the unbound components, extracted from MD trajectories, according to the procedure fully described in Materials and Methods. As shown in [Table 4](#), this analysis highlighted that compound **3** should be more active than the other two compounds, mainly due to an increase of the electrostatic contribution that could be due to the stable interaction with T342, which compensates the absence of the secondary interaction with K299. Conversely, compound **2** was predicted to be less potent than reference compound **VS6**, probably because it showed an interaction with T342 similar to that observed for **VS6** and the loss of the secondary interaction with K299.

Compounds **2** and **3** were commercially available and were thus purchased and tested for their Fyn inhibitory activity. Interestingly, in agreement with the computational studies, compound **2** showed an  $IC_{50}$  higher than  $100\ \mu\text{M}$ , whereas compound **3** displayed a nearly sixfold increase of activity with respect to **VS6** with an  $IC_{50}$  in the submicromolar range. In order to compare the binding mode predicted for compound **3** with respect to **PP2**, the reference inhibitor was docked into Fyn catalytic site by applying the same computational procedure used for the other compounds reported in this paper. As shown in [Figure S3](#) in the [Supplementary Material](#), the aminopyrimidine ring of **PP2** well matches the triazinone core of compound **3** and the two ligands share the H-bonds with the backbone of E343 and M345. On the contrary, the aniline moiety of **PP2** is not able to assume a disposition allowing the formation of the H-bond with the side chain of T342 predicted for compound **3**. Nevertheless, the *p*-chlorophenyl ring of **PP2** perfectly fills the predominantly hydrophobic pocket constituted by M318, I340, T342 and the side chains of K299 and E314, thus forming several additional lipophilic interactions with respect to the cyclohexyl ring of compound **3**. Moreover, the tert-butyl group of **PP2** forms further hydrophobic interactions with L277, V285 and L397 that are not observed for compound **3**.

Compound **3** was further tested in *in vitro* experiments to evaluate its antiproliferative potencies on cancer cells and **PP2** was used as a reference compound. To this aim, two tumour cell lines were chosen, the human non-small-cell lung A549 and the highly invasive human breast MDA-MB-231 cancer cells, due to the critical role that Fyn plays in the tumour progression and development of metastases in these two types of tumors<sup>46,47</sup>. Overall, compound **3** produced an appreciable inhibition of cell viability, with  $IC_{50}$  values ranging from 35 to  $101\ \mu\text{M}$  ([Table 5](#)) that

**Table 5.** Cell growth inhibitory activities (IC<sub>50</sub>) of compounds **3** and **PP2**.

Cancer cell line	Tissue of origin	IC <sub>50</sub> values (μM)	
		3	PP2
A549	Lung	101.0 ± 10.8	14.3 ± 2.0
MDA-MB-231	Breast	34.8 ± 4.6	12.0 ± 1.4

were lower than those showed by **VS6** (IC<sub>50</sub> = 145.0 and 198.2 for A549 and MDA-MB-231, respectively)<sup>20</sup>.

In conclusion, according to our consensus docking and MD simulation results, we can confirm the reliability of the binding mode predicted for compound **VS6** within Fyn catalytic site. In addition, the replacement of the benzodioxole moiety with a cyclohexyl ring led to compound **3** endowed with a six-fold increased activity and highlighted the role of the H-bond between the ligand and residue T342. Finally, compound **3**, tested on human cancer cell lines, proved to inhibit cell proliferation with an appreciable antiproliferative activity (IC<sub>50</sub> from 35 to 101 μM).

### Disclosure statement

No potential conflict of interest was reported by the authors.

### Funding

We are grateful to the University of Pisa (Progetti di Ricerca di Ateneo, PRA-2017–51) for funding.

### ORCID

Carlotta Granchi  <http://orcid.org/0000-0002-5849-0722>  
 Flavio Rizzolio  <http://orcid.org/0000-0002-3400-4363>  
 Filippo Minutolo  <http://orcid.org/0000-0002-3312-104X>  
 Tiziano Tuccinardi  <http://orcid.org/0000-0002-6205-4069>

### References

- Saito YD, Jensen AR, Salgia R, Posadas EM. Fyn: a novel molecular target in cancer. *Cancer* 2010;116:1629–37.
- Osterhout DJ, Wolven A, Wolf RM, et al. Morphological differentiation of oligodendrocytes requires activation of Fyn tyrosine kinase. *J Cell Biol* 1999;145:1209–18.
- Schafer I, Muller C, Luhmann HJ, White R. MOBP levels are regulated by Fyn kinase and affect the morphological differentiation of oligodendrocytes. *J Cell Sci* 2016;129:930–42.
- Lim SH, Kwon SK, Lee MK, et al. Synapse formation regulated by protein tyrosine phosphatase receptor T through interaction with cell adhesion molecules and Fyn. *EMBO J* 2009;28:3564–78.
- Palacios EH, Weiss A. Function of the Src-family kinases, Lck and Fyn, in T-cell development and activation. *Oncogene* 2004;23:7990–8000.
- Posadas EM, Al-Ahmadie H, Robinson VL, et al. FYN is over-expressed in human prostate cancer. *BJU Int* 2009;103:171–7.
- Charpin C, Secq V, Giusiano S, et al. A signature predictive of disease outcome in breast carcinomas, identified by quantitative immunocytochemical assays. *Int J Cancer* 2009;124:2124–34.
- Huang RY, Wang SM, Hsieh CY, Wu JC. Lysophosphatidic acid induces ovarian cancer cell dispersal by activating Fyn kinase associated with p120-catenin. *Int J Cancer* 2008;123:801–9.
- Singh MM, Howard A, Irwin ME, et al. Expression and activity of Fyn mediate proliferation and blastic features of chronic myelogenous leukemia. *PLoS One* 2012;7:e51611.
- Palacios-Moreno J, Foltz L, Guo A, et al. Neuroblastoma tyrosine kinase signaling networks involve FYN and LYN in endosomes and lipid rafts. *PLoS Comput Biol* 2015;11:e1004130.
- Elias D, Ditzel HJ. Fyn is an important molecule in cancer pathogenesis and drug resistance. *Pharmacol Res* 2015;100:250–4.
- Lee G, Thangavel R, Sharma VM, et al. Phosphorylation of tau by fyn: implications for Alzheimer's disease. *J Neurosci* 2004;24:2304–12.
- Schenone S, Brullo C, Musumeci F, et al. Fyn kinase in brain diseases and cancer: the search for inhibitors. *Curr Med Chem* 2011;18:2921–42.
- Hanke JH, Gardner JP, Dow RL, et al. Discovery of a novel, potent, and Src family-selective tyrosine kinase inhibitor. Study of Lck- and FynT-dependent T cell activation. *J Biol Chem* 1996;271:695–701.
- Peckham H, Giuffrida L, Wood R, et al. Fyn is an intermediate kinase that BDNF utilizes to promote oligodendrocyte myelination. *Glia* 2016;64:255–69.
- Mao LM, Wang JQ. Dopamine D2 receptors are involved in the regulation of Fyn and metabotropic glutamate receptor 5 phosphorylation in the rat striatum in vivo. *J Neurosci Res* 2016;94:329–38.
- Ko HM, Lee SH, Kim KC, et al. The role of TLR4 and Fyn interaction on lipopolysaccharide-stimulated PAI-1 expression in astrocytes. *Mol Neurobiol* 2015;52:8–25.
- Bain J, Plater L, Elliott M, et al. The selectivity of protein kinase inhibitors: a further update. *Biochem J* 2007;408:297–315.
- Poli G, Martinelli A, Tuccinardi T. Computational approaches for the identification and optimization of Src family kinases inhibitors. *Curr Med Chem* 2014;21:3281–93.
- Poli G, Tuccinardi T, Rizzolio F, et al. Identification of new Fyn kinase inhibitors using a FLAP-based approach. *J Chem Inf Model* 2013;53:2538–47.
- Maestro, version 9.0. Portland (OR): Schrödinger Inc; 2009. Available from: <https://www.schrodinger.com/>
- Macromodel, version 9.7. Portland (OR): Schrödinger Inc; 2009. Available from: <https://www.schrodinger.com/>
- Tuccinardi T, Poli G, Romboli V, et al. Extensive consensus docking evaluation for ligand pose prediction and virtual screening studies. *J Chem Inf Model* 2014;54:2980–6.
- Poli G, Martinelli A, Tuccinardi T. Reliability analysis and optimization of the consensus docking approach for the development of virtual screening studies. *J Enzym Inhib Med Ch* 2016;31:167–73.
- Granchi C, Caligiuri I, Bertelli E, et al. Development of terphenyl-2-methyloxazol-5(4H)-one derivatives as selective reversible MAGL inhibitors. *J Enzym Inhib Med Ch* 2017;32:1240–52.
- Morris GM, Huey R, Lindstrom W, et al. AutoDock4 and AutoDockTools4: automated docking with selective receptor flexibility. *J Comput Chem* 2009;30:2785–91.
- DOCK, version 6.7. San Francisco (CA): Molecular Design Institute, University of California; 1998. Available from: <http://dock.compbio.ucsf.edu/>
- FRED, version 3.0.0. Santa Fe (NM): OpenEye Scientific Software, Inc.; 2013. Available from: <https://www.eyesopen.com/>

29. OMEGA, version 2.4.6. Santa Fe (NM): OpenEye Scientific Software, Inc.; 2013. Available from: <https://www.eyesopen.com/>
30. Hawkins PC, Skillman AG, Warren GL, et al. Conformer generation with OMEGA: algorithm and validation using high quality structures from the Protein Databank and Cambridge Structural Database. *J Chem Inf Model* 2010;50:572–84.
31. Hawkins PC, Nicholls A. Conformer generation with OMEGA: learning from the data set and the analysis of failures. *J Chem Inf Model* 2012;52:2919–36.
32. Verdonk ML, Cole JC, Hartshorn MJ, et al. Improved protein-ligand docking using GOLD. *Proteins* 2003;52:609–23.
33. Glide, version 5.0. Portland (OR): Schrödinger Inc; 2009. Available from: <https://www.schrodinger.com/>
34. Trott O, Olson AJ. AutoDock Vina: improving the speed and accuracy of docking with a new scoring function, efficient optimization, and multithreading. *J Comput Chem* 2010;31:455–61.
35. Korb O, Monecke P, Hessler G, et al. pharmACOPhore: multiple flexible ligand alignment based on ant colony optimization. *J Chem Inf Model* 2010;50:1669–81.
36. Tuccinardi T, Poli G, Dell'Agnello M, et al. Receptor-based virtual screening evaluation for the identification of estrogen receptor beta ligands. *J Enzym Inhib Med Chem* 2015;30:662–70.
37. Kinoshita T, Matsubara M, Ishiguro H, et al. Structure of human Fyn kinase domain complexed with staurosporine. *Biochem Biophys Res Commun* 2006;346:840–4.
38. Case DA, Berryman JT, Betz RM, et al. AMBER, version 14. San Francisco (CA): University of California; 2015. Available from: <http://ambermd.org/>
39. York DM, Darden TA, Pedersen LG. The effect of long-range electrostatic interactions in simulations of macromolecular crystals - a comparison of the Ewald and truncated list methods. *J Chem Phys* 1993;99:8345–8.
40. Kollman PA, Massova I, Reyes C, et al. Calculating structures and free energies of complex molecules: combining molecular mechanics and continuum models. *Acc Chem Res* 2000;33:889–97.
41. Cincinelli R, Cassinelli G, Dallavalle S, et al. Synthesis, modeling, and RET protein kinase inhibitory activity of 3- and 4-substituted beta-carboline-1-ones. *J Med Chem* 2008;51:7777–87.
42. Tuccinardi T, Granchi C, Iegre J, et al. Oxime-based inhibitors of glucose transporter 1 displaying antiproliferative effects in cancer cells. *Bioorg Med Chem Lett* 2013;23:6923–7.
43. Poli G, Giuntini N, Martinelli A, Tuccinardi T. Application of a FLAP-consensus docking mixed strategy for the identification of new fatty acid amide hydrolase inhibitors. *J Chem Inf Model* 2015;55:667–75.
44. Dal Piaz F, Vera Saltos MB, Franceschelli S, et al. Drug affinity responsive target stability (DARTS) identifies laurifolioside as a new clathrin heavy chain modulator. *J Nat Prod* 2016;79:2681–92.
45. Petrou A, Geronikaki A, Terzi E, et al. Inhibition of carbonic anhydrase isoforms I, II, IX and XII with secondary sulfonamides incorporating benzothiazole scaffolds. *J Enzym Inhib Med Chem* 2016;31:1306–11.
46. Kostic A, Lynch CD, Sheetz MP. Differential matrix rigidity response in breast cancer cell lines correlates with the tissue tropism. *PLoS One* 2009;4:e6361.
47. Green TP, Fennell M, Whittaker R, et al. Preclinical anticancer activity of the potent, oral Src inhibitor AZD0530. *Mol Oncol* 2009;3:248–61.